crystals

MDPI

Article

First Principles Study on the Thermodynamic and Elastic Mechanical Stability of Mg_2X (X = Si,Ge) Intermetallics with (anti) Vacancy Point Defects

Yuhong Zhao *, Jinzhong Tian, Guoning Bai, Leting Zhang and Hua Hou

School of Materials Science and Engineering, North University of China, Taiyuan 030051, China; b1503001@st.nuc.edu.cn (J.T.); s1803004@st.nuc.edu.cn (G.B.); yxm0351@nuc.edu.cn (L.Z.); houhua@nuc.edu.cn (H.H.)

* Correspondence: zhaoyuhong@nuc.edu.cn

Received: 4 February 2020; Accepted: 11 March 2020; Published: 23 March 2020

Abstract: In this paper, based on the density functional theory, through thermodynamic and mechanical stability criteria, the crystal cell model of intermetallic compounds with vacancy and anti-site point defects is constructed and the lattice constant, formation heat, binding energy, elastic constant, and elastic modulus of Mg_2X (X = Si, Ge) intermetallics with or without point defects are calculated. The results show that the difference in the atomic radius leads to the instability and distortion of crystal cells with point defects; Mg_2X are easier to form vacancy defects than anti-site defects on the X (X = Si, Ge) lattice site, and form anti-site defects on the Mg lattice site. Generally, the point defect is more likely to appear at the Mg position than at the Si or Ge position. Among the four kinds of point defects, the anti-site defect x_{Mg} is the easiest to form. The structure of intermetallics without defects is more stable than that with defects, and the structure of the intermetallics with point defects at the Mg position is more stable than that at the Si/Ge position. The anti-site and vacancy defects will reduce the material's resistance to volume deformation shear strain, and positive elastic deformation, and increase the mechanical instability of the elastic deformation of the material. Compared with the anti-site point defect, the void point defect can lead to the mechanical instability of the transverse deformation of the material and improve the plasticity of the material. The research in this paper is helpful for the analysis of the mechanical stability of the elastic deformation of Mg_2X (X = Si, Ge) intermetallics under the service condition that it is easy to produce vacancy and anti-site defects.

Keywords: Intermetallic compounds; Thermodynamic stability; Elastic mechanical stability; Mg_2X (X = Si, Ge); Vacancy point defects; First principle method

1. Introduction

Mg_2X (X = Si, Ge) intermetallics have such advantages as high-temperature resistance, good corrosion resistance, high hardness, high conductivity, high-temperature electric potential and low thermal conductivity, etc.; and have important application prospects in the fields of metal matrix composite materials, structural materials, thermoelectric materials, battery materials, hydrogen storage devices, etc. [1–3]. At present, the theoretical research on it mainly focuses on structure stability, electronic structure, mechanical properties, and thermodynamic properties, and so on. According to the first principles and molecular dynamics, the structure, elasticity, and thermodynamic properties of Mg_2Si were predicted in Reference [4–6]. The effects of strain, deformation and high pressure on the electronic, optical, and thermoelectric properties of Mg_2Si have been calculated in reference [7–10]. Hirayama [11,12] theoretically studied the influence of doping on the structural parameters of Mg_2Si.

The lattice structure, mechanical properties, and phase transitions Mg_2X (X = Si, Ge) have been studied in Reference [13–17]. Reference [18–21] studied the electronic structure of doping defects of Mg_2X (X = Si, Ge and Sn) anti-fluorine compounds. References [22–24] used the first principle to calculate the interface structure of Mg_2Si and related compounds. Kessair [25] studied the structural characteristics of seven different types of Mg_2Si and found that the thermoelectric potential of cubic CaF_2 structure is very high, which may be the preferred material in thermoelectric applications. Vacancy point defects play a decisive role in the physical properties of thermoelectric materials and are used as a new way to improve thermoelectric properties. However, there are few studies on the structures of Mg_2X (X = Si, Ge) with vacancy and anti-site defects.

Therefore, in this paper, the equilibrium lattice constant, formation heat, binding energy, and elastic constant of Mg_2X (X = Si, Ge) system with vacancy defect structure are calculated by Density Functional Theory (DFT). The effect of vacancy defect on the structure and properties of Mg_2X (X = Si, Ge) intermetallics is explored from the microscopic point of view.

2. Computational Method

In this paper, based on the density functional theory (DFT) [26,27], we use the CASTEP [28] module in Materials Studio 8.0. The exchange-correlation potential was in the form of Perdew–Burke–Ernzerh (PBE) of the generalized gradient approximation (GGA) [29,30]. Considering computational accuracy and efficiency [31], the final cutoff energy of plane wave E_{cut} was set to be 380 eV. The Brillouin zone integral is in the form of 8 × 4 × 8 monkhorst-pack [32], and the super soft pseudopotential of the reciprocal space is selected as the potential function [33].

The parameter conditions are set as follows: the total energy of the system converges within 5.0 × 10^{-6} ev/atom, the force on each atom is less than 0.01 eV/Å, the stress deviation is lower than 0.02 GPa, the tolerance deviation is less than 5 × 10^{-4} Å.; the maximum convergence tolerance of energy and self-consistent field (SCF) convergence threshold are 5.0 × 10^{-6} eV/atom and 5.0 × 10^{-7} eV/atom, respectively. Both Mg_2Si and Mg_2Ge belong to the face-centered cubic (FCC) structure of anti-fluorite (CaF_2).

In this paper, we use 1 × 1 × 2 and 2 × 2 × 2 supercell models, so that we can more easily verify whether the calculated data is reasonable, and can compare the influence of different supercell sizes on the calculation results. The 1 × 1 × 2 $Mg_{16}X_8$ supercell crystals are shown in Figure 1. There are two vacancy defects V_{mg}, V_x, two anti-site defects Mg_X, X_{Mg} in the crystals, and the small red box indicates the location of the point defect.

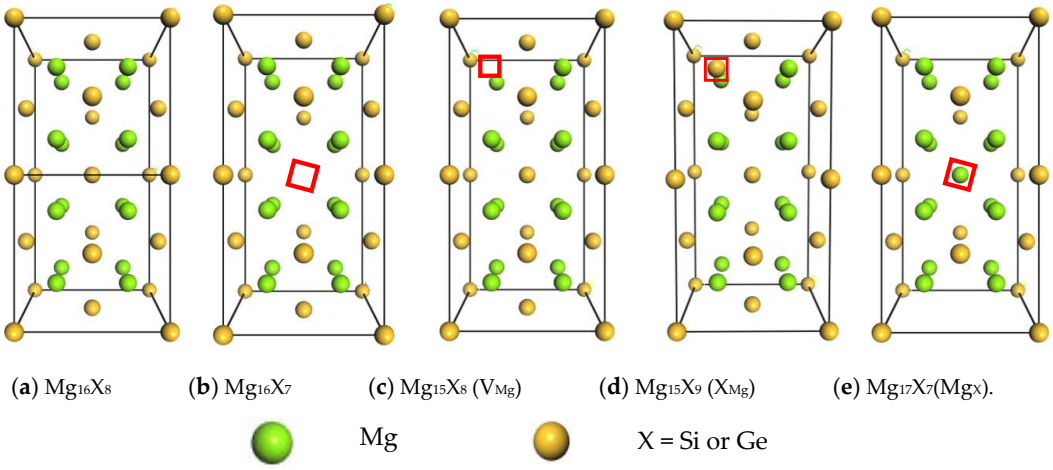

Figure 1. 1 × 1 × 2 supercell crystal structure of Mg_2X (X = Si, Ge) with vacancy point defects or anti-site defects, (**a**) $Mg_{16}X_8$, (**b**) $Mg_{16}X_7$ (V_X), (**c**) $Mg_{15}X_8$ (V_{Mg}), (**d**) $Mg_{15}X_9$ (X_{Mg}), and (**e**) $Mg_{17}X_7$ (Mg_X). The red squares represent the position of the vacancy or anti-site defects.

The 2 × 2 × 2 supercell model with 96 atoms is shown in Figure 2. The small red circle indicates the position of point defect, and the point defect concentration is reduced to a quarter of the former. We have made some comparative studies with the related calculation results of 1 × 1 × 2 supercells in this work.

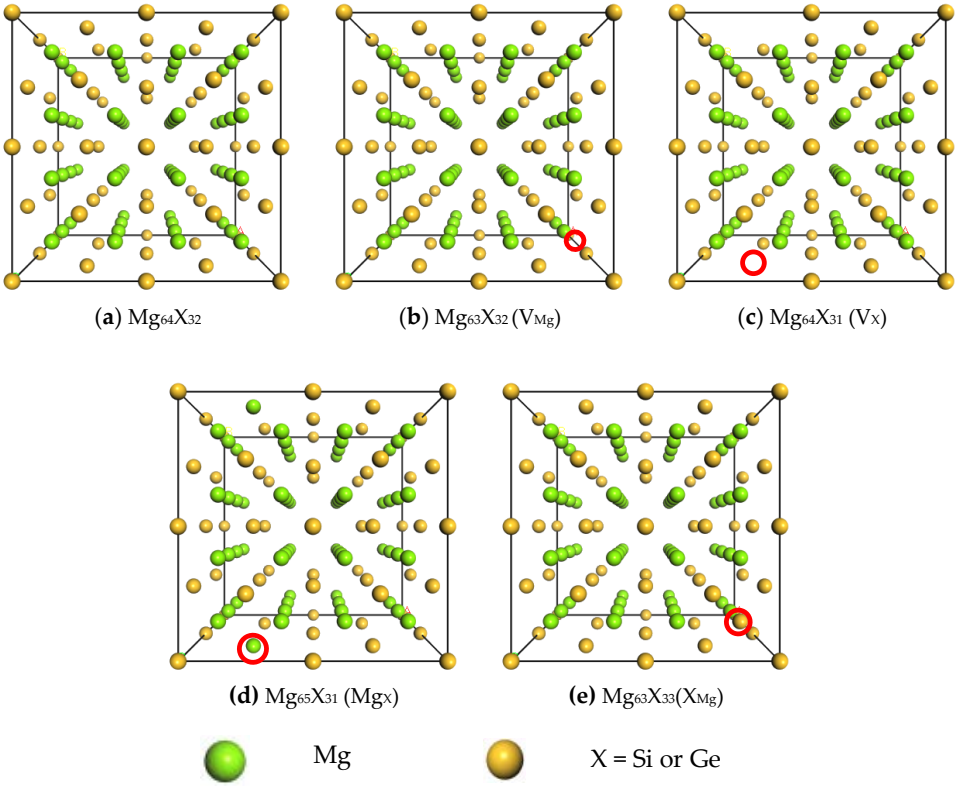

Figure 2. 2 × 2 × 2 supercell crystal structure of Mg_2X (X = Si, Ge) with vacancy point defects or anti-site defects, (**a**) $Mg_{64}X_{32}$, (**b**) $Mg_{63}X_{32}$ (V_{Mg}), (**c**) $Mg_{64}X_{31}$ (V_X), (**d**) $Mg_{65}X_{31}$ (Mg_X) and (**e**) $Mg_{63}X_{33}$ (X_{Mg}). The red squares represent the position of the vacancy or anti-site defects.

3. Results and Discussion

3.1. Equilibrium Lattice Stability of Intermetallics with or without Point Defects

The equilibrium lattice constants of Mg_2X (X = Si, Ge) intermetallic compounds have been calculated and shown in Table 1.

Table 1. Calculated equilibrium lattice constants of 1 × 1 × 2 Mg_2X (X = Si, Ge) cells with or without two types of point defects.

Intermetallics	a (Å)	b (Å)	c (Å)	V (Å^3)
$Mg_{16}Si_8$	6.351	6.351	12.702	512.338
$Mg_{16}Si_7(V_{Si})$	6.380	6.380	12.764	519.551
$Mg_{15}Si_8(V_{Mg})$	6.372	6.372	12.758	518.005
$Mg_{15}Si_9(Si_{Mg})$	6.369	6.369	12.962	525.793
$Mg_{17}Si_7(Mg_{Si})$	6.405	6.405	13.140	539.056
$Mg_{16}Ge_8$	6.385	6.385	12.770	520.586
$Mg_{16}Ge_7(V_{Ge})$	6.434	6.434	12.793	529.584
$Mg_{15}Ge_8(V_{Mg})$	6.427	6.427	12.872	531.695
$Mg_{15}Ge_9(Ge_{Mg})$	6.447	6.447	12.894	535.924
$Mg_{17}Ge_7(Mg_{Ge})$	6.464	6.464	13.229	552.751

The lattice constants of $Mg_{16}Si_8$ and $Mg_{16}Ge_8$ with point defects are listed in Table 1, and Figure 2 is the comparison of lattice constants of Mg_2X (X = Si, Ge) with point defects. It can be seen from Table 1 that the equilibrium lattice constants calculated in this paper are very close to the experimental values [34,35], which shows that the method adopted is reliable. It also can be seen from Table 1 that when the cell contains vacancy or anti vacancy point defects, lattice distortion occurs in the cell, resulting in cell expansion and a lattice constant increase. At the same time, as shown in Figure 3, the lattice constant of $Mg_{16}Ge_8$ with vacancy and anti-site defects is larger than that of $Mg_{16}Si_8$, which is due to the following relationship between the relative atomic radius: R_{Si} (0.118 nm) < R_{Ge} (0.123 nm) < R_{Mg} (0.160 nm).

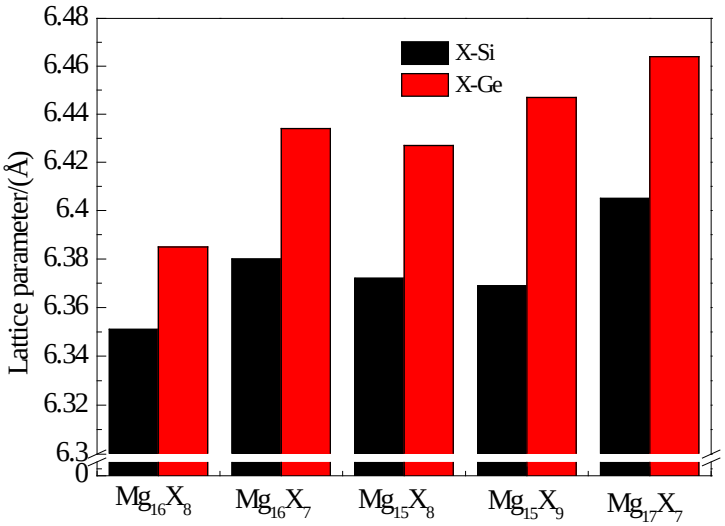

Figure 3. Comparison of lattice constants of Mg_2X (X = Si, Ge) with point defects.

The calculated results of lattice parameters of 1 × 1 × 2 supercells and 2 × 2 × 2 supercells (as shown in Table 2) are compared, and the results are consistent.

Table 2. Calculated equilibrium lattice constants of 2 × 2 × 2 Mg_2X (X = Si, Ge) cells with or without two types of point defects.

Intermetallics	A = b = c (Å)	V (Å^3)	Intermetallics	a = b = c (Å)	V (Å^3)
$Mg_{64}Si_{32}$	12.741	2068.290	$Mg_{64}Ge_{32}$	12.771	2083.054
$Mg_{64}Si_{31}(V_{Si})$	12.761	2078.015	$Mg_{64}Ge_{31}(V_{Ge})$	12.870	2131.974
$Mg_{63}Si_{32}(V_{Mg})$	12.768	2081.463	$Mg_{63}Ge_{32}(V_{Mg})$	12.879	2136.209
$Mg_{63}Si_{33}(Si_{Mg})$	12.760	2077.480	$Mg_{63}Ge_{33}(Ge_{Mg})$	12.884	2138.745
$Mg_{65}Si_{31}(Mg_{Si})$	12.808	2100.947	$Mg_{65}Ge_{31}(Mg_{Ge})$	12.918	2155.592

3.2. Effects of Vacancy and Anti-Site Points Defects on Thermodynamic Stability

The smaller the bond energy is, the less energy is needed to break the bond, the easier it is to be broken, the more unstable it is, so the harder it is to generate. The larger the bond energy is, the more energy is needed to destroy the bond. The less likely the bond is to be destroyed, the more stable the bond is, and the easier the crystal formed by the bond is. The calculation formula of the formation heat of $Mg_{16}X_8$ (X = Si, Ge) intermetallics with point defects is [36]:

$$\Delta H_f = \frac{E_{tot}^{AB} - N_A E_{solid}^{A} - N_B E_{solid}^{B}}{N_A + N_B} \quad (1)$$

where, E_{tot}^{AB} represents the average total energy of each crystal cell of Mg_2X intermetallic compound, N indicates the number of atoms in the crystal cell, and E_{solid}^{A}, E_{solid}^{B} represent the ground state energy of each atom in the solid cell, $E_{solid}^{Mg} = -973.95$ eV, $E_{solid}^{Si} = -107.26$ eV, and $E_{solid}^{Ge} = -107.29$ eV.

The binding energy E_{coh} of a crystal is the energy needed to decompose the crystal into a single atom, which is usually negative. Therefore, the larger the absolute value of the binding energy, the higher the stability of the intermetallics. The calculation formula of binding energy is [37]:

$$E_{coh} = \frac{E_{tot}^{AB} - N_A E_{atom}^{A} - N_B E_{atom}^{B}}{N_A + N_B} \quad (2)$$

where, E_{atom}^{AorB} represents the energy of each atom in the crystal cell in the free state, $E_{atom}^{Mg} = -972.48$ eV, $E_{atom}^{Si} = -101.85$ eV and $E_{atom}^{Ge} = -102.71$ eV.

The calculated formation heat and binding energy of Mg_2X (X = Si, Ge) cells with or without point defects are listed in Table 3. The more negative ΔH_f of the crystal is, the easier it is to form. That is to say, the absolute ΔH_f of the crystal is larger, it is not easy to be damaged, and it is easier to form.

Table 3. Computed formation heat (ΔH_f) and binding energy (E_{coh}) of $Mg_{16}X_8$ and $Mg_{64}X_{32}$ (X=Si, Ge) with or without (anti) vacancy point defects.

$1 \times 1 \times 2$ Intermetallics	ΔH_f (eV/atom)	E_{coh} (eV/atom)	$2 \times 2 \times 2$ Intermetallics	ΔH_f (eV/atom)	E_{coh} (eV/atom)
$Mg_{16}Si_8$	−0.180	−3.113	$Mg_{64}Si_{32}$	−0.170	−2.949
$Mg_{16}Si_7(V_{Si})$	−0.084	−2.911	$Mg_{64}Si_{31}(V_{Si})$	−0.148	−2.899
$Mg_{15}Si_8(V_{Mg})$	−0.092	−3.078	$Mg_{63}Si_{32}(V_{Mg})$	−0.155	−2.947
$Mg_{17}Si_7(Mg_{Si})$	−0.072	−2.852	$Mg_{65}Si_{31}(Mg_{Si})$	−0.142	−2.880
$Mg_{15}Si_9(Si_{Mg})$	−0.108	−3.103	$Mg_{63}Si_{33}(Si_{Mg})$	−0.155	−2.945
$Mg_{16}Ge_8$	−0.281	−2.953	$Mg_{64}Ge_{32}$	−0.259	−2.761
$Mg_{16}Ge_7$(VGe)	−0.167	−2.756	$Mg_{64}Ge_{31}(V_{Ge})$	−0.236	−2.716
$Mg_{15}Ge_8$(VMg)	−0.197	−2.910	$Mg_{63}Ge_{32}(V_{Mg})$	−0.248	−2.761
$Mg_{17}Ge_7(Mg_{Ge})$	−0.155	−2.708	$Mg_{65}Ge_{31}(Mg_{Ge})$	−0.230	−2.700
$Mg_{15}Ge_9(Ge_{Mg})$	−0.211	−3.002	$Mg_{63}Ge_{33}(Ge_{Mg})$	−0.248	−2.753

As shown in Table 3 that the absolute value of ΔH_f of Mg_2X (X = Si, Ge) with point defects is less than that without point defects, which means that the structure with point defects is easy to be destroyed, and it is easy to be in an unstable state before formation, that is to say; it is difficult to form compounds (For example, it can forms a stable structure with point defects at 0 K and 0 GPa, and the formed structure may become unstable under the influence of external factors, which is not contradictory to the relationship between binding energy and crystal stability in the following section of this paper).

It can also be seen from Table 3 that on the X (X = Si, Ge) lattice site, the absolute value of ΔH_f of intermetallic compounds with vacancy defects is larger than that with anti-site defects, indicating that the metal bond energy with vacancy defects on the X lattice site is larger than that with anti-site defects, and it is not easy to be damaged, and it is easier to form crystals, that is to say, intermetallic compounds are easier to form vacancy defects than anti-site on the X (X = Si, Ge) lattice site. However, Mg_2X is easier to form anti-site defects on the Mg lattice site.

It is also found that for $1 \times 1 \times 2$ Mg_2Si intermetallics, the ΔH_f (−0.092 eV/atom) of vacancy point defects at Mg position is smaller than that at Si position (−0.084 eV/atom), the absolute value is larger, and it is not easy to be destroyed, so it is easier to form; The formation energy (−0.108 eV/atom) of the anti-site defect at Mg position is smaller than that at Si position (−0.072 eV/atom), the absolute value is larger, it is not easy to be damaged, and it is easier to form, which indicates that the point defect is more likely to appear at the Mg position than at the Si position; The same analysis shows that for Mg_2Ge intermetallics, point defects are more likely to form at the Mg position than at the Ge

position. From Table 3, we can also find that this conclusion is also applicable to $Mg_{64}X_{32}$ (X = Si, Ge) intermetallics with 2 × 2 × 2 supercells.

It is also found that no matter 1 ×1× 2 supercells or 2 × 2 × 2 supercells, the absolute value of the binding energy of the intermetallics without point defects is higher than that of the intermetallics with point defects, which indicates that the energy required for atom bonding is higher and the structure is more stable when there is no defect. For the same type of defects, the absolute value of the binding energy at the Mg position is larger than that at the Si/Ge position, so the structure of the intermetallics forming point defects at the Mg position is more stable than that at the Si/Ge position.

The defect formation energies of vacancy and anti-site can be calculated by the following expression:

$$\Delta E_f = E_{total}(defect) - E_{total}(perfect) - \sum_i \Delta n_i \mu_i \quad (3)$$

where, $E_{total}(perfect)$ and $E_{total}(defect)$ represent the total energy of perfect supercell and defect supercell of Mg_2X (X = Si, Ge), respectively; n_i represent the number of atoms added or removed in Mg_2X (X = Si, Ge) intermetallics, μ_i represent the corresponding chemical potential of the atom, i.e., the defect formation energies of vacancy and anti-site in Mg_2X (X = Si, Ge) are shown in Table 4.

Table 4. Computed $\Delta E_f{}^{vac}$ and $\Delta E_f{}^{anti}$ of $Mg_{16}X_8$ and $Mg_{64}X_{32}$ (X = Si, Ge) with vacancy and anti-site point defects.

Intermetallics		$\Delta E_f{}^{vac}$ (eV/atom)		$\Delta E_f{}^{anti}$ (eV/atom)	
		ΔE_{Mg}^{vac}	$\Delta E_x{}^{vac}$	ΔE_{Mg}^{vati}	$\Delta E_x{}^{anti}$
1 × 1 × 2	$Mg_{16}Si_8$	3.68	7.82	−2.23	6.57
	$Mg_{16}Ge_8$	3.45	7.24	−1.68	5.90
2 × 2 × 2	$Mg_{64}Si_{32}$	3.09	7.67	−2.55	6.62
	$Mg_{64}Ge_{32}$	2.77	7.02	−2.10	5.83

As shown in Table 4, for Mg_2X (X = Si, Ge), the ΔE^{vac} and ΔE^{anti} at the Si or Ge position is bigger than that at the Mg position, which indicates that the point defect is more likely to appear at Mg position than at Si or Ge position. Among the four kinds of point defects, the defect forming energy of the anti-site defect ΔE_{Mg}^{anti} is the smallest, which indicates that the anti-site defect x_{Mg} is the easiest to form in Mg_2X. Compared with other point defects, the ΔE_{Mg}^{anti} is negative, which means it can form spontaneously in 1 × 1 × 2 and 2 × 2 × 2 supercells. The defect formation of vacancy ΔE^{vac} and inversion ΔE^{anti} (except Mg_{Si}) in Mg_2X (X = Si, Ge) can decrease with the increase of supercell size, which shows that only the anti-site defect Mg_{Si} is easy to form in 1 × 1 × 2 supercells, while other point defects tend to form in 2 × 2 × 2 supercell.

3.3. Effects of Vacancy and Anti-Site Points Defects on Elastic Mechanical Stability

3.3.1. Elastic Constants of Stability Criteria

Elastic constants are used to measure the ability of materials to resist external force and deformation and can be used to predict the mechanical stability of materials. To determine the elastic stability of a crystal, three independent elastic constants [38] are needed for the cubic structure: C_{11}, C_{12}, C_{44}. For tetragonal structures, six independent elastic constants [39] are needed: $C_{11}, C_{12}, C_{13}, C_{33}, C_{44}, C_{66}$. In this paper, Mg_2X (X = Si, Ge) cells with point defects belong to tetragonal structure, and Mg_2X (X = Si, Ge) cells without point defects belong to cubic structure [40,41].

The calculated elastic constants of Mg_2X (X = Si, Ge) cells with (without) point defects are listed in Table 5. It can be seen that our calculation results are close to others' theoretical calculation results [42], indicating that the selection of the parameters is reasonable.

Table 5. Computed elastic constants C_{ij} (GPa) of Mg_2X (X = Si, Ge) with or without a point defect (a vacancy or an anti-site defect) in different supercells.

Supercell	Intermetallics	C_{11}	C_{12}	C_{13}	C_{33}	C_{44}	C_{66}
-	**Mg_2Si**	**113.40**	**22.71**	**-**	**-**	**45.09**	-
-	Cal. [42]	114.07	19.56	-	-	33.32	-
$1 \times 1 \times 2$	$Mg_{16}Si_7(V_{Si})$	91.55	27.67	21.98	94.37	19.64	28.76
	$Mg_{15}Si_{8(}V_{Mg})$	90.70	27.25	29.12	89.98	29.91	33.24
	$Mg_{17}Si_7(Mg_{Si})$	91.83	24.34	25.26	84.48	38.07	31.50
	$Mg_{15}Si_9(Si_{Mg})$	100.74	27.37	27.37	97.76	29.78	30.69
$2 \times 2 \times 2$	$Mg_{64}Si_{31}(V_{Si})$	103.94	24.76			32.46	
	$Mg_{63}Si_{32}(V_{Mg})$	105.98	25.23			38.96	
	$Mg_{63}Si_{33}(Si_{Mg})$	107.95	23.45			39.83	
	$Mg_{65}Si_{31}(Mg_{Si})$	102.69	25.95			36.64	
-	**Mg_2Ge**	**105.32**	**20.83**	**-**	**-**	**42.58**	**105.32**
-	Cal. [43]	107.3	21.1	-	-	41.8	107.3
$1 \times 1 \times 2$	$Mg_{16}Ge_7(V_{Ge})$	86.30	24.62	19.36	89.24	22.13	86.30
	$Mg_{15}Ge_8(V_{Mg})$	84.38	25.08	26.89	83.96	29.24	84.38
	$Mg_{17}Ge_7(Mg_{Ge})$	83.71	21.32	25.99	80.78	32.83	83.71
	$Mg_{15}Ge_9(Ge_{Mg})$	94.53	25.42	24.64	92.92	30.48	94.53
$2 \times 2 \times 2$	$Mg_{64}Ge_{31}(V_{Ge})$	98.69	22.22			32.46	
	$Mg_{63}Ge_{32}(V_{Mg})$	98.05	23.14			37.08	
	$Mg_{63}Ge_{33}(Ge_{Mg})$	103.14	22.97			38.42	
	$Mg_{65}Ge_{31}(Mg_{Ge})$	95.57	23.53			34.59	

In the case of cubic crystals, the conditions of elastic stability are well known [43]:

$$C_{11} - C_{12} > 0;\ C_{11} + 2C_{12} > 0;\ C_{44} > 0 \tag{4}$$

The elastic Born stability criteria for the tetragonal system are [43]:

$$C_{11} > |C_{12}|;\ 2C_{13}^2 \langle C_{33}(C_{11} + C_{12});\ C_{44} \rangle 0;\ C_{66} > 0 \tag{5}$$

Based on the computed elastic constants, the effects of point defects on the mechanical stability of Mg_2X (X = Si, Ge) intermetallics can be evaluated. Obviously, the elastic constants C_{ij} calculated in Table 3 meet the mechanical stability criteria. Therefore, the Mg_2X (X = Si, Ge) intermetallic compounds with and without vacancy or anti-vacancy point defects are all mechanically stable structures.

3.3.2. Elastic Modulus of Mechanical Stability

The yield limit σ_s and strength limit σ_b obtained in the tensile test reflect the bearing capacity of the material to the force, while the elongation δ or section shrinkage ψ reflect the plastic deformation capacity of the material. In order to express the difficulty of material resisting deformation in the elastic range, the meaning of material elastic modulus E is usually reflected by the rigidity of parts in practical engineering, because once the parts are designed according to the stress, the rigidity is judged by the deformation generated by the load in the service process in the elastic deformation range. Generally, the load-causing unit strain is the rigidity of the part. For example, for tension and compression parts, the rigidity is EA_0, and A_0 is the cross-section area of the part. It can be seen that in order to improve the stiffness EA_0 of the parts, which is to reduce the elastic deformation of the parts, the materials with high elastic modulus can be selected, and the cross-sectional area A_0 of the bearing can be appropriately increased. The importance of stiffness is that it determines the stability of parts in service, especially for slender rod-shaped parts and thin-walled parts. Therefore, for the theoretical analysis and design calculation of components, the elastic modulus E is an important mechanical performance index that is often used.

Elastic modulus E is defined as the ratio of stress to corresponding strain when the ideal material has small deformation. The nature of modulus depends on the nature of deformation. Elastic modulus E (unit: GPa) includes the Young's modulus E (tensile stress/tensile strain, also called positive elastic modulus, tensile modulus), shear modulus G (shear stress/shear strain angle), compression modulus K (compressive stress/shrinkage strain), bulk modulus B (bulk pressure/bulk strain)—the reciprocal of the modulus is called the flexibility expressed in J. When it is not easy to cause confusion, the elastic modulus of general metal materials refers to the young's modulus, that is, the positive elastic modulus.

From the macroscopic point of view, the modulus of elasticity is a measure of the ability of an object to resist elastic deformation. From the microscopic point of view, it is a reflection of the bonding strength among atoms, ions, or molecules. All the factors that affect the bonding strength can affect the elastic modulus of the material, such as bonding mode, crystal structure, chemical composition, microstructure, temperature, etc. The young's modulus E of metal materials will fluctuate by 5% or more due to different alloy compositions, heat treatment state and cold plastic deformation. However, generally speaking, the elastic modulus of metal material is a mechanical property index that is not sensitive to the structure. Alloying, heat treatment (fiber structure), cold plastic deformation, and other factors have little influence on the elastic modulus E, and the external factors such as temperature and loading rate have little influence on it, so the elastic modulus E is regarded as a constant in general engineering application.

Poisson's ratio ν refers to the ratio of the absolute value of the transverse positive strain and the positive axial strain when the material is under tension or compression in a single direction, also known as the transverse deformation coefficient, which is the elastic constant reflecting the transverse deformation of the material. When the material extends (or shortens) along the load direction, it will also shorten (or lengthen) in the direction perpendicular to the load. The negative value of the ratio of the strain ε_l in the vertical direction to the strain ε in the load direction is called Poisson's ratio of the material, i.e., $\nu = -\varepsilon_l/\varepsilon$. Poisson's ratio ν of materials is generally determined by test method. For traditional materials, ν is generally constant in the elastic working range, but beyond the elastic range, ν increases with the increase of stress until $v = 0.5$. For the material with large Poisson's ratio, the amount of transverse deformation is larger than that of the longitudinal deformation after the material is stressed and before plastic deformation, otherwise, the amount of transverse deformation is smaller than that of the longitudinal deformation.

In Table 6, we compare the results of calculation when there are vacancy point defects in different supercells of Mg_2X (X = Si, Ge) intermetallic compounds; it is found that for Mg_2Si type intermetallics, the B, G, and E of Mg_2X with Mg vacancy (V_{Mg}) are higher than those of Mg_2X with X vacancy (V_X). The above results show that the vacancy defects in Mg position, compared with those in the Si position and Ge position, will lead to the stronger resistance to volume deformation, shear strain and elastic deformation of crystal materials, the greater the rigidity, the less deformation, the stronger the brittleness and the worse the plasticity.

For intermetallic compounds with anti-site point defects, the B, G and E of Mg_2X (X = Si, Ge) with the X_{Mg} anti-site are higher than those of Mg_2X with the Mg_X anti-site, indicating that when the Si or Ge atom replace the Mg atom to form anti-vacancy defects, compared with Mg atom replacing Si or Ge atom to form anti vacancy defect, the material has a strong resistance to volume deformation, shear strain and elastic deformation, but poor plasticity. Besides, for Mg_2X (X = Si, Ge) with same point defect structure, the B, G, and E of $1 \times 1 \times 2$ supercells are smaller than those of $2 \times 2 \times 2$ supercells, which indicates that the Mg_2X (X = Si, Ge) with point defects are easier to form in $2 \times 2 \times 2$ supercells. Therefore, the point defects generated on the Mg position of $2 \times 2 \times 2$ supercells can enhance the mechanical stability of the material, while the plasticity is poor.

Table 6. Lists the calculated bulk modulus, B.; the shear modulus, G.; Young's modulus, E.; Poisson's ratio ν and G/B.

Supercell	Intermetallics	*B*/GPa	*G*/GPa	*E*/GPa	G/B	ν
-	**Mg_2Si**	52.94	45.19	105.54	0.854	0.168
-	Cal. [42]	51.06	46.12	108.35	0.903	0.150
$1 \times 1 \times 2$	$Mg_{16}Si_7(V_{Si})$	46.74	27.33	68.62	0.585	0.255
	$Mg_{15}Si_{8(}V_{Mg})$	49.15	31.00	76.85	0.631	0.239
	$Mg_{17}Si_7(Mg_{Si})$	46.38	34.41	82.77	0.742	0.202
	$Mg_{15}Si_9(Si_{Mg})$	51.49	35.53	83.61	0.752	0.239
$2 \times 2 \times 2$	$Mg_{64}Si_{31}(V_{Si})$	51.16	35.14	85.79	0.687	0.221
	$Mg_{63}Si_{32}(V_{Mg})$	52.15	39.52	94.65	0.758	0.198
	$Mg_{65}Si_{31}(Mg_{Si})$	51.53	37.32	90.19	0.724	0.208
	$Mg_{63}Si_{33}(Si_{Mg})$	51.62	40.78	96.84	0.790	0.187
-	**Mg_2Ge**	**49.00**	**42.45**	**98.81**	**0.866**	**0.164**
-	Cal. [43]	49.80	42.30	98.90	0.847	-
$1 \times 1 \times 2$	$Mg_{16}Ge_7(V_{Ge})$	43.48	28.17	69.50	0.648	0.234
	$Mg_{15}Ge_8(V_{Mg})$	45.47	29.51	72.79	0.649	0.233
	$Mg_{17}Ge_7(Mg_{Ge})$	43.88	30.16	73.62	0.688	0.220
	$Mg_{15}Ge_9(Ge_{Mg})$	47.28	32.76	79.84	0.693	0.219
$2 \times 2 \times 2$	$Mg_{64}Ge_{31}(V_{Ge})$	47.71	34.66	83.71	0.727	0.208
	$Mg_{63}Ge_{32}(V_{Mg})$	48.11	37.23	88.78	0.774	0.193
	$Mg_{65}Ge_{31}(Mg_{Ge})$	47.54	35.15	84.61	0.739	0.203
	$Mg_{63}Ge_{33}(Ge_{Mg})$	49.69	39.08	92.88	0.786	0.189

Table 6 also shows that the Poisson's ratio ν (0.168 and 0.164) of **$Mg_{16}X_8$** without point defects is the smallest, and the Poisson's ratio ν with defects is larger (greater than 0.18), indicating that the formation of defects makes the transverse deformation of the material larger and the transverse elastic mechanical instability increased. It was also found that the Poisson's ratio of Mg_2X (X = Si, Ge) with X vacancy is higher than that of Mg_2X with the Mg_X anti-site. Similarly, the Poisson's ratio of Mg_2X with Mg vacancy was slightly higher than that of Mg_2X with X_{Mg} anti-site. Thus, the above results show that when there are defects in the Mg, Si, and Ge position, the void point defects increase the instability of transverse deformation more than the anti-void point defects. Note that for Mg_2X (X = Si, Ge) with the same point defect structure (except Mg_{Si}), the Poisson's ratio ν of the $2 \times 2 \times 2$ supercells is smaller than that of the $1 \times 1 \times 2$ supercells, indicating that the point defects in larger supercells can only increase the instability of transverse deformation slightly, compared with $1 \times 1 \times 2$ supercells.

According to Pugh's report [44], G/B can predict the ductility or brittleness of materials, and materials with G/B value higher than the critical value of 0.57 belong to brittle materials; it can be seen from Table 6 that both Mg_2X (X = Si, Ge) with and without point defects are brittle materials. The maximum G/B value of Mg_2X without point defects indicates that the formation of defects will improve the ductility of materials; the G/B value of vacancy point defects is smaller than that of anti-site defects, indicating that vacancy point defects can improve the plasticity of materials more than anti-site defects. Compared with $2 \times 2 \times 2$ supercells, the G/B of Mg_2X with the same point defect structure (except Mg_{Si}) in $1\times 1 \times 2$ supercells can enhance the plasticity of materials.

In theory, only two of the three elastic constants E, G and ν of isotropic materials are independent, because they have the following relationship: $G = E/[2\,(1+\nu)]$. This is consistent with the essence of the definition of Poisson's ratio. For anisotropic materials, the elastic modulus in x, y and z directions, shear modulus and Poisson's ratio in xy, xz, and yz planes are required

3.3.3. Elastic Anisotropy

Anisotropy exists widely in all kinds of materials. In short, crystals have different properties in different directions. It is easy to confuse anisotropy and inhomogeneity, which are two completely different concepts. Anisotropy means that the properties of materials are related to directions, while inhomogeneity means that the properties of materials are related to parts. In the case of single crystals, at any point in the interior, the structures and properties are the same, but it has different performance in different directions.

Crystal is anisotropic, with different properties in different directions, and has strict symmetry. Here, the symmetry is a very remarkable property, which is widely used in mathematics and physics, and also commonly used in the analysis of material properties. Polycrystalline materials have preferred orientation and certain anisotropy.

All kinds of materials are elastic, and the elastic properties of most materials are anisotropic [45,46]. For example, in cubic crystals, the [111] direction is usually more difficult to compress than the [100] direction. The three-dimensional surface Young"s modulus E of intermetallics is calculated as follows [47]

$$\frac{1}{E} = S_{11} - 2\left(S_{11} - S_{12} - \frac{S_{44}}{2}\right)\left(l_1^2 l_2^2 + l_2^2 l_3^2 + l_1^2 l_3^2\right) \quad (6)$$

where S_{11}, S_{12}, and S_{44} represent the flexibility coefficient, l_1, l_2, and l_3 indicate direction cosines relative to the x, y, and z directions, respectively.

Figures 4 and 5 show the three-dimensional Young's modulus E surface of each intermetallic compound Mg_2X (X = Si, Ge) at 0 GPa with $1 \times 1 \times 2$ supercells and $2 \times 2 \times 2$ supercells, respectively. The near sphere shows that these intermetallic compounds are elastic and anisotropic [48]. Compared with other point defects of Mg_2X, the Mg_2X with X vacancy exhibits a relatively obvious deviation from spherical shape, which indicates that the Mg_2X with X vacancy has a relatively strong anisotropy. The degree of spherical deviation of Mg_2X decreases with the increase of supercell size, implying that Mg_2X with point defects show a relatively weak anisotropy in the $2 \times 2 \times 2$ supercells.

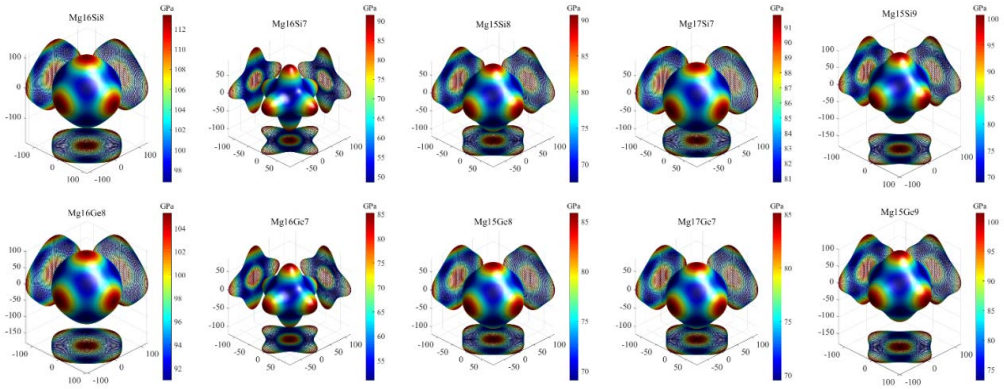

Figure 4. Computed 3D Young's modulus E (GPa) of Mg_2X (X=Si, Ge) Intermetallics in the 1×1×2 supercells.

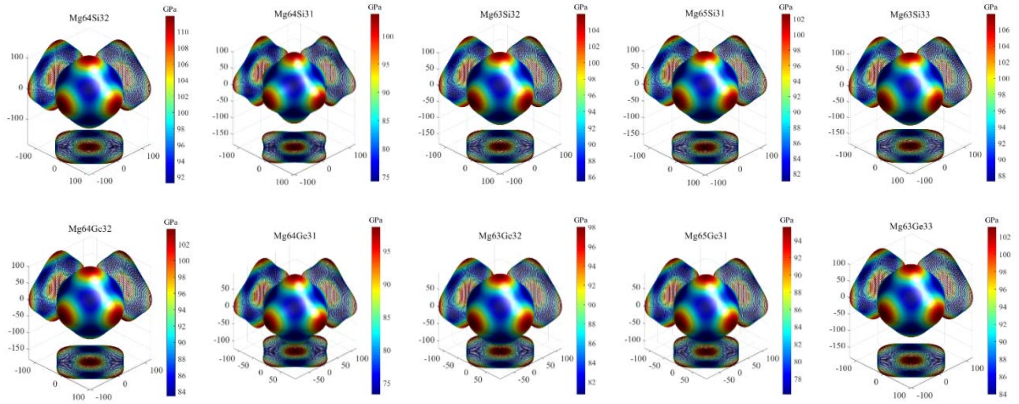

Figure 5. Computed 3D Young's modulus E (GPa) of Mg_2X (X = Si, Ge) intermetallics in the 2 × 2 × 2 supercells.

4. Conclusions

In this paper, based on DFT, the influence of point defects on the structure and elastic mechanical stability of Mg_2X (X = Si, Ge) intermetallic is revealed from the microscopic point of view:

(1) The difference of atomic radius, the lattice constant of Mg_2Ge type intermetallics with (without) point defects is larger than that of Mg_2Si type, and the existence of point defects leads to the instability of crystal cells and the expansion of lattice distortion.

(2) The predicted ΔH_f and E_{coh} are consistently negative for all Mg_2X (X = Si, Ge) with point defects, implying the thermodynamic stability of Mg_2X (X = Si, Ge) with point defects. The absolute value of ΔH_f of Mg_2X (X = Si, Ge) with point defects is smaller than that of the cells without point defects, which indicates that the structure with point defects is relatively difficult to form; intermetallics are easier to form vacancy defects than anti-site on the X (X = Si, Ge) lattice site and form anti-site defects on the Mg lattice site; the ΔH_f of the vacancy or anti-site defects of Mg_2X at the Si or Ge position is bigger than that at the Mg position, which indicates that the point defect is more likely to appear at the Mg position than at the Si or Ge position; the absolute value of the binding energy of the intermetallics without point defects is higher than that of the intermetallics with point defects, which indicates that the energy required for atom bonding is higher and the structure is more stable when there is no defect; the structure of the intermetallics forming point defects at the Mg position is more stable than that at the Si/Ge position.

(3) When the point defects exist, the bulk modulus B, shear modulus G and Young's modulus E of intermetallic compounds become smaller, which indicates that the void and anti-void point defects will reduce the volume deformation resistance, shear strain resistance, and positive elastic deformation resistance of materials, and increase the mechanical instability of elastic deformation of materials. When there is a vacancy or anti-site defect in the Mg position, the resistance to volume deformation, shear strain and elastic deformation of the crystal is stronger than that in the Si or Ge position. Therefore, the point defects in the Mg position enhance the mechanical stability of the material, while the plasticity is poor. The maximum G/B value of Mg_2X without point defects indicates that the formation of defects will improve the ductility of materials; the G/B value of vacancy point defects is smaller than that of anti-site defects, indicating that vacancy point defects can improve the plasticity of materials more than anti-site defects.

(4) The Poisson's ratio v of Mg_2X without point defects is the smallest, which indicates that the formation of defects makes the transverse deformation of the material larger, and the transverse elastic instability increased. Compared with 2 × 2 × 2 supercells, the G/B of Mg_2X with the same point defect structure (except Mg_{Si}) in 1 × 1 × 2 supercells can enhance the plasticity of materials.

Author Contributions: Conceptualization, Y.Z. and L.Z.; methodology, Y.Z. and J.T.; software, G.B. and J.T.; validation, Y.Z, G.B. and L.Z.; formal analysis, H.H. and G.B.; investigation, L.Z.; resources, Y.Z. and H.H.; data

curation, G.B. and Y.Z.; writing—original draft preparation, Y.Z.; writing—review and editing, Y.Z. and J.T.; visualization, G.B.; supervision, Y.Z.; project administration, Y.Z.; funding acquisition, Y.Z. and H.H. All authors have read and agreed to the published version of the manuscript.

Funding: This research was funded by National Natural Science Foundation of China (Nos. 51774254, 51774253, 51701187, 51674226, 51804279, 51801189); The Science and Technology Major Project of Shanxi Province (No. 20191102008); Platform and Talent Project of Shanxi Province (No. 201805D211036); Guiding Local Science and Technology Development Projects by the Central Government (No. YDZX20191400002796); Transformation of Scientific and Technological Achievements Special Guide Project of Shanxi Province (No. 201804D131039).

Conflicts of Interest: The authors declare no conflict of interest.

References

1. Cheng, P.; Zhao, Y.H.; Lu, R.P.; Hou, H.; Bu, Z.Q.; Yan, F. Effect of Ti addition on the microstructure and mechanical properties of cast Mg-Gd-Y-Zn alloys. *Mater. Sci. Eng. A* **2017**, *708*, 482–491. [CrossRef]
2. Bell, L.E. Cooling, heating, generating power, and recovering waste heat with thermoelectric systems. *Science* **2008**, *321*, 1457–1461. [CrossRef] [PubMed]
3. Vantomme, A.; Mahan, J.E.; Langouche, G.; Becker, J.P.; Van Bael, M.; Temst, K.; Van Haesendonck, C. Thin film growth of semiconducting Mg_2Si by codeposition. *Appl. Phys. Lett.* **1997**, *70*, 1086–1088. [CrossRef]
4. Yu, R.; Li, G.; Guo, X.; Deng, K.Q.; Pang, A.M.; Zhai, P.C. An improved interatomic potential function for thermoelectric Mg_2Si: A combination study of ab-initio and molecular dynamics method. *Comput. Mater. Sci.* **2018**, *149*, 49–56. [CrossRef]
5. Liu, X.; Wang, Y.; Sofo, J.O.; Zhu, T.; Chen, L.Q.; Zhao, X. First-principles studies of lattice dynamics an-d thermal properties of $Mg_2Si_{1-x}Sn_x$. *J. Mater. Res.* **2015**, *30*, 2578–2584. [CrossRef]
6. Gu, X.; Li, X.; Yang, R. Phonon transmission across $Mg_2Si/Mg_2Si_{1-x}Sn_x$ interfaces: A first-principles-base-d atomistic Green's function study. *Phys. Rev. B* **2015**, *91*, 205313. [CrossRef]
7. Kaur, K.; Dhiman, S.; Kumar, R. Strain engineering on thermoelectric performance of Mg_2Si. *Mater. Res. Express* **2017**, *4*, 075509. [CrossRef]
8. Chen, Q.; Xie, Q.; Zhao, F.J.; Cui, D.; Li, X. First-principles calculations of electronic structure and optic-al properties of strained Mg_2Si. *Chin. Sci. Bull.* **2010**, *55*, 2236–2242. [CrossRef]
9. Huan, T.D.; Tuoc, V.N.; Le, N.B.; Minh, N.V.; Woods, L.M. High-pressure phases of Mg_2Si from first principles. *Phys. Rev. B* **2016**, *93*, 094109. [CrossRef]
10. Jun, L.W.; Lin, J.Z.; Qi, J.L.; Yuan, Z.C.; Ru, S.; Zhu, H.; Xiu, R.L. Pressure-induced metallization transition in Mg_2Ge. *Acta Phys. Sin.* **2017**, *66*, 166201. [CrossRef]
11. Hirayama, N.; Iida, T.; Morioka, S.; Sakamoto, M.; Nishio, K.; Kogo, Y. First-principles investigation of structural, electronic, and thermoelectric properties of n-and p-type Mg_2Si. *J. Mater. Res.* **2015**, *30*, 2564–2577. [CrossRef]
12. Hirayama, N.; Iida, T.; Funashima, H.; Morioka, S.; Sakamoto, M.; Nishio, K.; Hamada, N. Theoretical analysis of structure and formation energy of impurity-doped Mg_2Si: Comparison of first-principles codes for material properties. *Jpn. J. Appl. Phys.* **2015**, *54*, 07JC05. [CrossRef]
13. Murtaza, G.; Sajid, A.; Rizwan, M.; Takagiwa, Y.; Khachai, H.; Jibran, M.; Omran, S.B. First principles study of Mg_2X (X = Si,Ge,Sn,Pb): Elastic, optoelectronic and thermoelectric properties. *Mater. Sci. Semicond. Proc.* **2015**, *40*, 429–435. [CrossRef]
14. Jund, P.; Viennois, R.; Colinet, C.; Hug, G.; Fèvre, M.; Tedenac, J.C. Lattice stability and formation energies of intrinsic defects in Mg_2Si and Mg_2Ge via first principles simulations. *J. Phys. Condens. Matter* **2012**, *25*, 035403. [CrossRef] [PubMed]
15. Chernatynskiy, A.; Phillpot, S.R. Anharmonic properties in Mg_2X (X = C,Si,Ge,Sn,Pb) from first-principles calculations. *Phys. Rev. B* **2015**, *92*, 064303. [CrossRef]
16. Guo, S.D. Electronic structure and thermoelectric properties of $(Mg_2X)_2/(Mg_2Y)_2$(X,Y = Si, Ge, Sn) superlattices from first-principle calculations. *Eur. Phys. J. B* **2016**, *89*, 134. [CrossRef]
17. Yu, F.; Sun, J.X.; Chen, T.H. High-pressure phase transitions of Mg_2Ge and Mg_2Sn: First-principles calculations. *Phys. B Condens. Matter* **2011**, *406*, 1789–1794. [CrossRef]
18. Pulikkotil, J.J.; Singh, D.J.; Auluck, S.; Saravanan, M.; Misra, D.K.; Dhar, A.; Budhani, R.C. Doping and temperature dependence of thermoelectric properties in Mg_2(Si, Sn). *Phys. Rev. B* **2012**, *86*, 155204. [CrossRef]

19. Zwolenski, P.; Tobola, J.; Kaprzyk, S. KKR–CPA study of electronic structure and relative stability of Mg_2X (X= Si, Ge, Sn) thermoelectrics containing point defects. *J. Alloy. Compd.* **2015**, *627*, 85–90. [CrossRef]
20. Liu, X.; Xi, L.; Qiu, W.; Yang, J.; Zhu, T.; Zhao, X.; Zhang, W. Significant roles of intrinsic point defects in Mg_2X (X = Si,Ge,Sn) thermoelectric materials. *Adv. Electron. Mater.* **2016**, *2*, 1500284. [CrossRef]
21. Viennois, R.; Jund, P.; Colinet, C.; Tédenac, J.C. Defect and phase stability of solid solutions of Mg_2X with an antifluorite structure: An ab initio study. *J. Solid State Chem.* **2012**, *193*, 133–136. [CrossRef]
22. Sun, J.; Li, C.; Liu, X.; Yu, L.; Li, H.; Liu, Y. Investigation on AlP as the heterogeneous nucleus of Mg_2Si in Al–Mg_2Si alloys by experimental observation and first-principles calculation. *Res. Phys.* **2018**, *8*, 146–152. [CrossRef]
23. Deng, Q.; Wang, Z.; Wang, S.; Shao, G. Simulation of planar Si/Mg_2Si/Si pin heterojunction solar cells for high efficiency. *Solar Energy* **2017**, *158*, 654–662. [CrossRef]
24. Xia, Z.; Li, K. First-principles study on Al_4Sr as the heterogeneous nucleus of Mg_2Si. *Mater. Res. Express* **2016**, *3*, 126503. [CrossRef]
25. Kessair, S.; Arbouche, O.; Amara, K.; Benallou, Y.; Azzaz, Y.; Zemouli, M.; Bouazza, B.S. First principles prediction of a new high-pressure phase and transport properties of Mg_2Si. *Indian J. Phys.* **2016**, *90*, 1403–1415. [CrossRef]
26. Burke, K. Perspective on density functional theory. *J. Chem. Phys.* **2012**, *136*, 150901. [CrossRef]
27. Perdew, J.P. Density-functional approximation for the correlation energy of the inhomogeneous electron gas. *Phys. Rev. B* **1986**, *33*, 8822. [CrossRef]
28. Segall, M.D.; Lindan, P.J.D.; Probert, M.J.; Pickard, C.J.; Hasnip, P.J.; Clark, S.J.; Payne, M.C. First-principles simulation: Ideas, illustrations and the CASTEP code. *J. Phys. Condens. Matter* **2002**, *14*, 2717. [CrossRef]
29. Vanderbilt, D. Soft self-consistent pseudopotentials in generalized eigenvalue formalism. *Phys. Rev. B* **1990**, *41*, 7892. [CrossRef]
30. Perdew, J.P.; Burke, K.; Ernzerhof, M. Generalized gradient approximation made simple. *Phys. Rev. Lett.* **1996**, *77*, 3865. [CrossRef]
31. Wen, Z.Q.; Hua, H.; Tian, J.Z.; Zhao, Y.H.; Li, H.J.; Han, P.D. First-principles investigation of martensitic transformation and magnetic properties of Ni_2XAl (X= Cr, Fe, Co) Heusler compounds. *Intermetallics* **2018**, *92*, 15–19. [CrossRef]
32. Zhao, Y.H.; Wang, S.; Zhang, B.; Yuan, Y.; Guo, Q.; Hou, H. The anisotropy of three-component medium entropy alloys in AlCoCrFeNi system: First-principle studies. *J. Solid State Chem.* **2019**, *276*, 232–237. [CrossRef]
33. Pack, J.D.; Monkhorst, H.J. "Special points for Brillouin-zone integrations"—A reply. *Phys. Rev. B* **1977**, *16*, 1748. [CrossRef]
34. Madelung, O. Numerical data and functional relationships in science and technology. *N. Ser.* **1982**, *New Series III (17)*, 571–619.
35. Rowe, D.M. *Thermoelectrics Handbook: Macro to Nano*; CRC Press: Boca Raton, FL, USA, 2005.
36. Zhao, Y.H.; Deng, S.; Liu, H.; Zhang, J.; Guo, Z.; Hou, H. First-principle investigation of pressure and temperature influence on structural, mechanical and thermodynamic properties of Ti_3AC_2 (A=Al and Si). *Comput. Mater. Sci.* **2018**, *154*, 365–370. [CrossRef]
37. Zhang, C.; Han, P.; Yan, X.; Wang, C.; Xia, L.; Xu, B. First-principles study of typical precipitates in creep resistant magnesium alloys. *J. Phys. D Appl. Phys.* **2009**, *42*, 125403. [CrossRef]
38. Duan, L.J.; Liu, Y.C. Relationships between Elastic Constants and EAM/FS Potential Functions for Cubic Crystals. *Acta Metall. Sin.* **2020**, *56*, 112–118. [CrossRef]
39. Boulet, P.; Verstraete, M.J.; Crocombette, J.P.; Crocombette, J.P.; Briki, M.; Record, M.C. Electronic properties of the Mg_2Si thermoelectric material investigated by linear-response density-functional theory. *Comput. Mater. Sci.* **2011**, *50*, 847–851. [CrossRef]
40. Hill, R. The elastic behavior of a crystalline aggregate. *Proc. Phys. Soc. Sect. A* **1952**, *65*, 349. [CrossRef]
41. Hou, H.; Wen, Z.; Zhao, Y.; Zhao, Y.; Fu, L.; Wang, N.; Han, P. First-principles investigations on structural, elastic, thermodynamic and electronic properties of Ni3X (X= Al, Ga and Ge) under pressure. *Intermetallics* **2014**, *44*, 110–115. [CrossRef]
42. Zhang, H.; Shang, S.; Saal, J.E.; Saengdeejing, A.; Wang, Y.; Chen, L.Q.; Liu, Z.K. Enthalpies of formation of magnesium compounds from first-principles calculations. *Intermetallics* **2009**, *17*, 878–885. [CrossRef]

43. Mouhat, F.; Coudert, F.X. Necessary and Sufcient Elastic Stability Conditions in Various Crystal Systems. *Phys. Rev. B* **2014**, *90*, 224104. [CrossRef]
44. Pugh, S.F. XCII. Relations between the elastic moduli and the plastic properties of polycrystalline pure metals. *Lond. Edinb. Dublin Philos. Mag. J. Sci.* **1954**, *45*, 823–843. [CrossRef]
45. Chung, D.H.; Buessem, W.R.; Vahldiek, F.W.; Mersol, S.A. *Anisotropy in Single Crystal Refractory Compounds*; Plenum: New York, NY, USA, 1968; p. 328.
46. Tian, J.Z.; Zhao, Y.H.; Hou, H.; Wang, B. The effect of alloying elements on the structural stability, mechanical properties, and Debye temperature of Al_3Li: A first-principles study. *Materials* **2018**, *11*, 1471. [CrossRef] [PubMed]
47. Nye, J.F. *Physical Properties of Crystals: Their Representation by Tensors and Matrices*; Oxford University Press: Oxford, UK, 1985. [CrossRef]
48. Tian, J.Z.; Zhao, Y.H.; Hou, H.; Han, P.D. First-principles investigation of the structural, mechanical and thermodynamic properties of Al2Cu phase under various pressure and temperature conditions. *Solid State Commun.* **2017**, *268*, 44–50. [CrossRef]